The Complex Core Level Spectra of CeO_2: An Analysis in Terms of Atomic and Charge Transfer Effects

P. S. Bagus[a], C. J. Nelin[b], E. S. Ilton[c], M. Baron[d], H. Abbott[d,e], E. Primorac[d], H. Kuhlenbeck[d,*], S. Shaikhutdinov[d], H.-J. Freund[d]

[a]*Department of Chemistry, University of North Texas, Denton, Texas 76203-5017, USA*
[b]*Maury's Trail, Austin, Texas 78730, USA*
[c]*Pacific Northwest National Laboratory, 902 Battelle Boulevard, P.O. Box 999, Richland, Washington 99352, USA*
[d]*Fritz-Haber-Institut der Max-Planck-Gesellschaft, Faradayweg 4-6, D-14195 Berlin, Germany*
[e]*Present address: Georgia Institute of Technology, Department of Chemistry and Biochemistry, 901 Atlantic Drive, Atlanta, Georgia 30322, USA*

Abstract

We present a rigorous *parameter-free* theoretical treatment of the Ce 4s and 5s photoelectron spectra of CeO_2. The currently accepted model explains the satellite structure in the photoelectron spectra in terms of mixed valence ($Ce\,4f^0\,O\,2p^6$, $Ce\,4f^1\,O\,2p^5$, and $Ce\,4f^2\,O\,2p^4$) configurations. We show that charge transfer (CT) into Ce 5d as well as configurations involving intra-atomic movement of charge must be considered in addition and compute their contributions to the spectra.

Introduction

Due to electronic many body interactions, X-ray photoelectron spectroscopy (XPS) data may exhibit complex fine structure, which carries information about the electronic structure. Insight into the origin of the spectral features will contribute significantly to an understanding of the electronic structure, especially of highly correlated materials where localized open d or f shells are present. In these cases, many-body effects of both intra- and inter-atomic origin are present. While these effects have been discussed for many years, there still is no agreement about the importance of the various mechanisms; see ref. 1 and references therein. For example, although the photoemission spectra of NiO have been studied for over 25 years [2–5], the origin of features in these spectra is still analyzed in recent papers [6, 7]. Another material with unusually complex spectra is CeO_2 [8] which

*Corresponding author
Email address: kuhlenbeck@fhi-berlin.mpg.de (H. Kuhlenbeck)

is of considerable interest for its catalytic properties [9]. A proper interpretation of the spectra could be important for understanding these properties. The theoretical studies to present [10, 11] have been based on parameterized Anderson model Hamiltonians where the spectral structures have been assigned to a mixing of Ce $4f^0$ O $2p^6$, Ce $4f^1$ O $2p^5$, and Ce $4f^2$ O $2p^4$ configurations [8, 10, 11]. Although the Anderson model has been used extensively to interpret the spectra of highly correlated oxides [12], agreement with experiment is normally established by adjusting parameters in the model and this adjustment may involve the neglect of important many-body effects [13].

Here, we present the results of a rigorous *ab initio* theoretical treatment of the Ce 4s and 5s XPS spectra of CeO_2, including relative energies, E_{rel}, and intensities, I_{rel}. For comparison, we also present experimental spectra for these regions. Our detailed analysis of the origins of the features in the 4s and 5s spectra shows that the assignment of the Ce core-level peaks to a superposition of configurations without CT ($4f^0$), single CT ($4f^1$), and double CT ($4f^2$) [8, 10, 11] is an oversimplification. Both spectra contain significant contributions of intra-atomic charge rearrangement and O 2p→Ce 5d charge-transfer. Given the general applicability of the many-body mechanisms considered [5, 13–16], it is reasonable to assume that the conclusions drawn here are also relevant for other core levels than those studied.

Theoretical and Experimental Details

The theory uses an embedded CeO_8 cluster and many-body effects are treated by mixing different configurations with configuration interaction, CI, wavefunctions, WF's. The WF's are fully relativistic where the 4-component spinors are variationally optimized separately for the initial and final state configurations so that account is taken of final state orbital relaxation [1]. The theoretical and computational methodologies are described in ref. 17. We represent the WF for the closed shell initial state with a single determinant [17]. The intra-atomic many-body effects for the final state WF's are included with configurations where the dominantly Ce spinors are redistributed over partly occupied orbitals [13, 15–17]; details of the intra-atomic many-body effects are discussed separately for the Ce 4s and 5s spectra. For the inter-atomic CT many-body effects, we included all symmetry allowed single CT configurations where an O 2p electron is transferred into a Ce 4f or 5d orbital. We also included a subset of double CT configurations where two O 2p electrons are transferred. Our tests indicate that increasing the number of these configurations will not lead to major changes in the theoretical spectra. This separation into intra-and inter-atomic many-body effects is possible because our optimized orbitals are dominantly localized on either the Ce cation or the O anions. Of course, there is covalent mixing of the O 2p ligand orbitals

with the nominally empty Ce 4f and 5d shells and this mixing is fully taken into account by our variational optimization. (See refs. 1 and 17 for discussion of this type of covalent mixing.) For the purpose of our analysis of the many-body effects, we view the orbitals as though they were fully localized. We have used a single set of orbitals to describe the configurations with and without CT since this dramatically simplifies the CI calculation [5, 18]. With our limited CI, which does not include a very large space of correlating orbitals [15, 19], the choice of a single set of orbitals will lead to ~1-3 eV uncertainties in E_{rel} [15, 20, 21]. While there are also uncertainties in the I_{rel}, there is evidence that they are much smaller than for the E_{rel} [22]. The I_{rel} are obtained with the Sudden Approximation, SA, [23, 24] and broadened to account for the inherent and experimental broadening of the XPS spectra; Gaussian broadening for the Ce 5s of 2.5 eV FWHM and for the 4s of 3.0 eV FWHM were used.

The experimental XPS spectra were recorded with a Scienta R4000 electron energy analyzer from a ~13 nm thick CeO_2(111) film which was grown on Ru(0001) according to a procedure described in ref. 25. Synchrotron radiation from the BESSY II electron storage ring in Berlin served to ionize the core levels. A Tougaard-type background was subtracted prior to plotting.

Results and Discussion

For the 5s spectrum, the envelope of the sum of all individual I_{rel}, as well as the individual final states with largest I_{rel}, is compared with experiment in Fig. 1. The main peaks of the theoretical and experimental spectra have been aligned but no other adjustments have been made. Each of the five theoretical features, labeled A-E in Fig. 1, can be associated with a feature in the experimental spectrum; for this association, we consider both the energies and intensities of the lines. Feature A, at E_{rel}~-5 eV is a weak shake-down satellite that can be seen to the right of the experimental main peak. Feature B, clearly associated with the main XPS peak, has important contributions from two states. The weak shake-up feature C is associated with the high BE shoulder of the XPS main peak. Feature D, at E_{rel}~10 eV has contributions from two states, which, see below, are related to the two states in the main peak B. Peak D is associated with the experimental satellite about 3.5 eV lower in BE where the theoretical error in E_{rel} arises because of the different contributions of CT configurations to the states in peaks B and D, see below. Finally, the weak Feature E at E_{rel}~15 eV has contributions from a few states and is associated with the broad XPS peak centered at somewhat smaller E_{rel}.

In Tables 1 and 2, we analyze the electronic structure of the states in the various peaks in terms of their CT character and in terms of the occupations of the relevant Ce and O orbitals. For all the features except B and D, we were able to

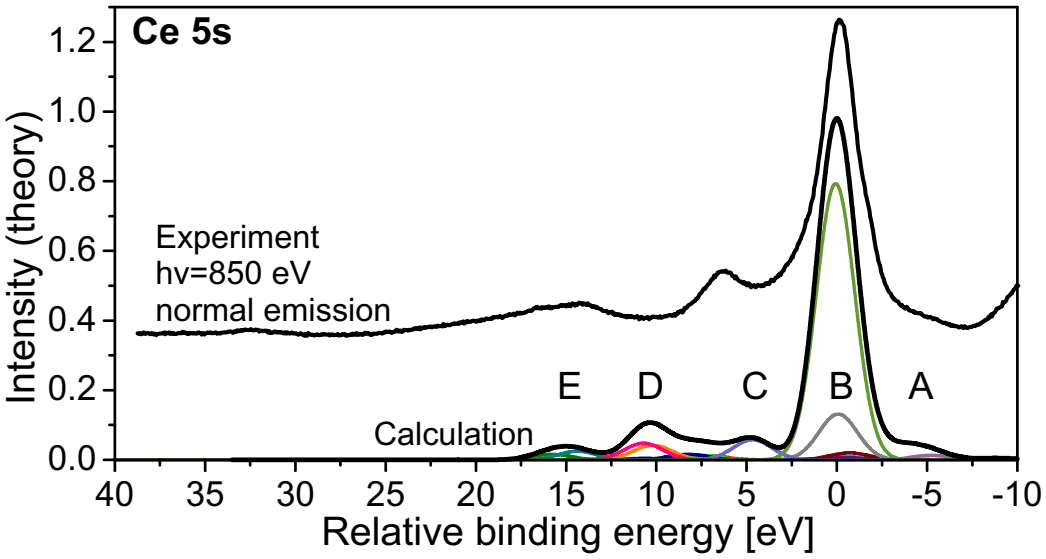

Figure 1: Theory and experiment for the 5s spectrum of CeO_2.

choose the state with the largest SA I_{rel} as being representative of all the states that contributed significantly to the feature. For features B and D, the two states with large I_{rel} have different electronic character and are discussed separately.

In Table 1, we give the weights of the configurations without CT, Wht(CT0), and with single CT, Wht(CT1). The deviation of Wht(CT0)+Wht(CT1) from 1.0, normally quite small, measures the involvement of double CT configurations. Our *ab initio* result that double CT is small is different from the semi-empirical results [10, 11], where double CT is very important, especially for the leading edge features. In our work, the state in the main peak at E_{rel}=0 that has the largest I_{rel} is composed of configurations without CT, 72%, and with single CT, 28%. The contribution of CT to this intense peak will allow states with a larger CT character to steal intensity from it [1, 13, 26]. The second state that contributes to the main peak, at E_{rel}=-0.1 eV has 20% of the intensity of the first state; it is dominated by single CT configurations, which comprise almost 90% of the WF. The states at E_{rel}=4.6 eV, feature C, and at E_{rel}=10.1 eV, one of the two states in feature D, have the smallest CT contributions and their intensity arises dominantly from atomic many-body effects. The remaining states are dominated by single CT configurations; thus features A and E arise from states with Wht(CT1)≈1.0.

A more detailed understanding of the character of the 5s-hole states can be obtained from the occupations of key orbitals in the CI WF's. These occupations are defined as the expectation values, of the number operators for the appropriate orbitals. The Ce occupations are N(5s), N(5p), N(5d), and N(4f). For the O 2p or-

Feature	E_{rel} (eV)	I_{rel}	Wht(CT0)	Wht(CT1)
A. Shake-down	-5.3	0.01	0.02	0.98
B. Main peak	-0.1	0.09	0.12	0.88
	+0.0	0.55	0.72	0.28
C. Shake-up	+4.6	0.04	0.96	0.04
D. Shake-up	+10.1	0.03	0.87	0.13
	+10.6	0.03	0.38	0.60
E. Shake-up	+14.3	0.02	0.03	0.96

Table 1: Analysis of the CT character of selected 5s-hole states of CeO_2. For each state, the E_{rel} and I_{rel} and the weights of configurations, Wht(CT0) and Wht(CT1), are given; see text.

bitals, the change from the full occupation of the 2p shell, ΔN(O-2p)<0, is given. The occupation numbers are integer for the XPS allowed configuration where a 5s electron is removed. The many-body effect of the mixing of XPS forbidden configurations with the XPS allowed configuration [1] leads to the strong deviations from integral N(i) seen in Table 2 for the state at E_{rel}=0.0. The atomic terms for the 5s-hole states involve redistribution of the 7 electrons in the $5s^1 5p^6$ configuration among the 5s, 5p, and 5d shells [13, 14, 27]. Of particular importance is the frustrated Auger configuration, FAC [13], where one 5p electron of the $5s^2 5p^4 5d^1$ configuration is dropped to fill the 5s shell and a second 5p is promoted into the 5d shell.

For the intense peak at E_{rel}=0.0 in feature B, the occupations in Table 2 show that both inter-atomic and intra-atomic redistributions of charge are present. While there is inter-atomic CT of 0.3 O 2p electrons into Ce 4f and Ce 5d, the intra-atomic redistribution can be seen from the fact that N(5p) is reduced by 0.4 electrons from its nominal value of 6 and N(5s) is increased by 0.35 electrons. A

Feature	E_{rel} (eV)	N(5s)	N(5p)	N(5d)	N(4f)	ΔN(O-2p)
A. Shake-down	-5.3	1.99	5.01	0.62	0.37	-0.98
B. Main peak	-0.1	1.89	5.10	0.78	0.12	-0.89
	+0.0	1.35	5.58	0.25	0.12	-0.29
C. Shake-up	+4.6	1.94	4.15	0.94	0.01	-0.04
D. Shake-up	+10.1	1.85	4.31	0.94	0.04	-0.13
	+10.6	1.37	5.26	0.60	0.42	-0.66
E. Shake-up	+14.3	1.03	5.95	0.99	0.03	-0.99

Table 2: The occupations of the Ce and O 2p orbitals, denoted N(nl) and ΔN(O-2p), in the WF's of the selected states shown in Table 1; see text. The E_{rel} are also given.

detailed analysis shows that ~2/3 of the loss of electrons from the Ce 5p shell arises from the atomic FAC excitation $5p^2 \rightarrow 5s5d$ and ~1/3 from configurations that couple CT from O 2p with moving a Ce 5p electron into the Ce 5s shell. The coupling of CT with dropping a 5p to fill the 5s shell leads to the shake-down satellite, feature A; see below. The contribution of the $5p^2 \rightarrow 5s5d$ excitation to the state at E_{rel}=0.0 leads to intensity for satellites where the WF is dominated by the spin-orbit split $5s^2 5p^4 5d^1$ configurations. The satellites are the states at E_{rel}=4.6 eV with N(5p)=4.15 and at E_{rel}=10.1 eV with N(5p)=4.3. On the other hand, the second state that contributes to feature D is dominated by CT configurations with a smaller weight from the atomic FAC configurations. This is also the case for the second state in feature B at E_{rel}=0.1 eV, which is dominated by CT from O 2p largely to Ce 5d coupled with ~0.9 Ce 5p electrons that move down to almost fill the 5s shell; see Table 2. The shake-down satellite at -5.3 eV, feature A, involves the motion of one 5p electron into the 5s shell together with CT of essentially one O 2p electron into the Ce 4f and 5d shells. Finally, the low intensity feature E at E_{rel}=14.3 eV is dominated by CT into the Ce 5d orbitals. For features A and E, CT into the Ce 5d shell is more important than into the Ce 4f shell.

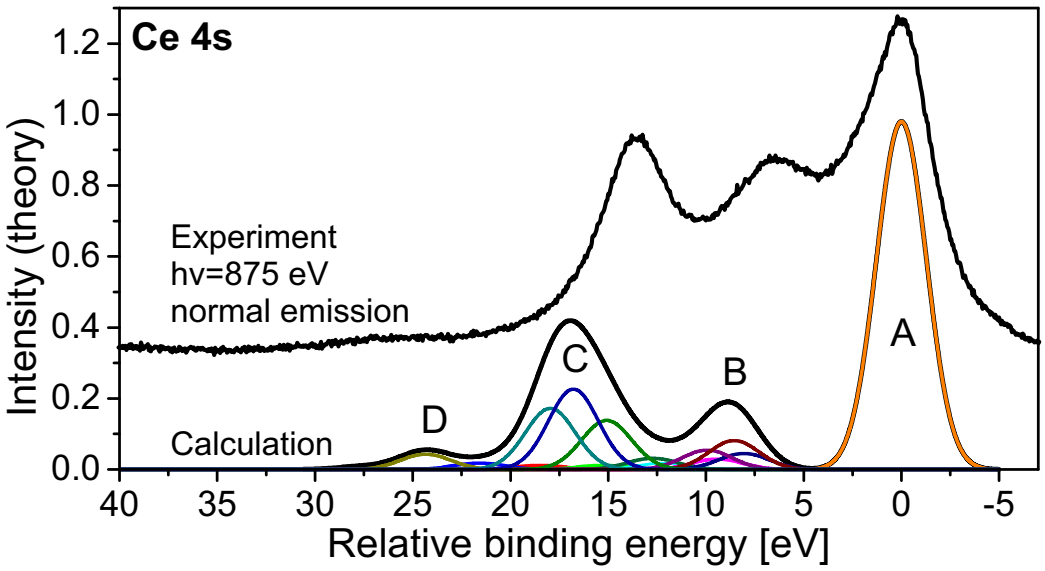

Figure 2: Theory and experiment for the 4s spectrum of CeO_2.

For the Ce 4s spectrum, as for the Ce 5s, single and double CT configurations are included in the CI WF's; however, the configurations that represent intra-atomic many-body effects are, of necessity different, from those of the Ce 5s case. The FAC that is analogous to the important $5p^2 \rightarrow 5s5d$ FAC for the 5s-hole states is not possible for the 4s-holes because the 4d shell is filled. However, a 4f FAC,

[13, 16] where a 4p electron drops into the 4s shell and a 4d is promoted into the empty 4f shell is included. This FAC significantly lowers the energy of the main 4s-hole peak but it leads to only weak satellites at high energy, E_{rel}~80 eV, because of the large differences among the energies of the Ce 4s, 4p, 4d, and 4f sub-shells. We have also included in the many-body CI for the 4s-hole states, the shake-down configurations that couple the atomic and CT effects by dropping a 4p electron into the 4s shell and transferring an O 2p electron into an unoccupied Ce shell. For the 5s spectrum, the 5p→5s plus CT coupling leads to shake-down peaks because these coupled configurations have energies within ≤10 eV of the XPS allowed 5s hole configuration. For the 4s spectrum, the larger splitting of the 4s and 4p energies leads to high excitation energies and, hence, to a much smaller importance of these coupled configurations.

The theoretical 4s spectrum is compared to experiment in Fig. 2 where the Gaussian broadened sum over all final states and the individual contributions of states with large I_{rel} are shown; as in Fig. 1, the experimental and theoretical peaks have been aligned. Three of the four theoretical features, labeled A to D, can be directly correlated to the XPS; the main peak and the two intense satellites reproduce the main experimental features. The calculated E_{rel} at features B and C are too large by ~3 eV because, with the single orbital set that we have used for our CI WF's, we do not treat the energies of CT configurations as accurately as those without CT [20–22]. As we show below, Feature A is dominated by CT0 configurations while features B and C are dominated by CT1 configurations and, hence, our computed E_{rel} are somewhat too large. Finally, it may be possible to associate the weak shake-up satellite at E_{rel}~24.5 eV with the intensity in the high BE tail of the XPS.

The main peak at E_{rel}=0, feature A, is dominated by the contribution of a single final ionic state while there are a few states contributing to each of features B, C, and D. However, the electronic characters of the different states contributing to features B to D are reasonably similar. Thus, it is sufficient to give the CT weights, Table 3, and the orbital occupations, Table 4, for a single representative state in the different spectral features. For each of the features, we choose the state

Feature	E_{rel} (eV)	I_{rel}	Wht(CT0)	Wht(CT1)
A. Main Peak	+0.0	0.43	0.95	0.01
B. Shake-up	+8.6	0.04	0.01	0.85
C. Shake-up	+16.8	0.10	0.01	0.83
D. Shake-up	+24.4	0.02	0.00	0.66

Table 3: Analysis of the CT character of selected 4s-hole states; see the cation to Table 1 and the text.

Feature	N(4s)	N(4p)	N(4d)	N(4f)	N(5d)	ΔN(O-2p)
A. Main Peak	1.10	5.90	9.90	0.19	0.00	-0.10
B. Shake-up	1.01	5.99	9.99	1.14	0.00	-1.13
C. Shake-up	1.00	6.00	10.00	1.13	0.02	-1.15
D. Shake-up	1.00	6.00	10.00	0.70	0.65	-1.34

Table 4: Occupations of the Ce and O 2p orbitals in the wavefunctions of the selected states for the 4s hole shown in Table 3; see text and caption to Table 2.

with the largest SA I_{rel}. For the 4s spectrum, data for E_{rel}, I_{rel}, and the weights of configurations with and without CT given in Table 3 parallel the 5s data presented in Table 1. For all the XPS features, Wht(CT0)+Wht(CT1) is close to 1.0 indicating that double CT, while not negligible, is not especially important for the hole state WF's. The low intensity feature D is an exception since double CT configurations comprise 1/3 of the WF for the representative state in Table 3. Feature A, the main peak at E_{rel}=0, is dominated by configurations without CT, while all the satellites are strongly dominated by CT configurations. Our results for the E_{rel} of the states dominated by CT and for the contribution of double CT configurations to the hole-state WF's are quite different from the semi-empirical Anderson model results [10, 11]. This raises serious questions about the validity of the Anderson model calculations [8, 10, 11]. The satellites for the 4s-hole carry considerably more intensity than for the 5s-hole; as can be seen from the main peak I_{rel} given in Tables 1 and 3. The sum of the I_{rel} for the two states contributing to the Ce 5s XPS main peak is 0.64 while the I_{rel} for the 4s main peak is 0.43. Since the I_{rel} for the 4s and 5s XPS are both normalized to 1, the difference shows that there is 50% greater satellite intensity in the 4s than in the 5s XPS.

Insight into the character of the 4s-hole states comes from the occupation numbers given in Table 4; these are as defined for the 5s-hole states. The Ce 4s, 4p, and 4d occupations change from the ideal values of 1, 6, and 10 because of atomic many body effects; i.e., from the 4f FAC as discussed above. Although, N(4f) can be >0 because of the 4f FAC and because of inter-atomic CT into Ce 4f; N(5d)>0 only because of CT. For the main peak, feature A, the atomic many body effects involve moving 0.1 4p electrons into the 4s shell and 0.1 4d electrons into the 4f shell. There is a CT of another 0.1 electrons from O 2p into the Ce 4f and there is no CT into Ce 5d. All of the 4s satellites are dominated by CT with very little intra-atomic contributions.

Conclusions

Our *ab initio* study of CeO_2 provides three conclusions that need to be taken into account for a correct description of the significance of the XPS spectra, especially as it allows insight into materials properties. First, it is necessary to take intra-atomic many-body effects into account as well as inter-atomic CT. Furthermore, the consequences of these intra-atomic many-body effects are quite different for the spectra of different shells. Second, the role of double CT is not as simple as assumed in previous semi-empirical studies. Finally, there is a new aspect of CT not previously taken into account, namely that the CT from O 2p can be either to Ce 4f or to Ce 5d. Our results suggest that the extent of the CT to the Ce 5d shell may depend on the core-level that is ionized with the CT for deeper core holes being dominated by CT to 4f while the CT to 5d is more important for shallower core holes. This might explain the different behavior for the CeO_2 4d and 3d spectra [8] and merits further investigation.

Acknowledgments

We acknowledge support by the Geosciences Research Program, Office of Basic Energy Sciences, U.S. DOE, the Alexander von Humboldt foundation, and the DFG through their SFB 546, Transition Metal Oxide Aggregates". Computer support from the Pittsburgh Supercomputer center is also acknowledged. A portion of the research was performed in the Environmental Molecular Sciences Laboratory at PNNL.

References

[1] P. S. Bagus, E. S. Ilton, Effects of covalency on the p-shell photoemission of transition metals: MnO, Phys. Rev. B 73 (2006) 155110.

[2] G. A. Sawatzky, J. W. Allen, Magnitude and origin of the band gap in NiO, Phys. Rev. Lett. 53 (1984) 2339.

[3] J. Zaanen, G. A. Sawatzky, J. W. Allen, Band gaps and electronic structure of transition-metal compounds, Phys. Rev. Lett. 55 (1985) 418.

[4] A. Fujimori, F. Minami, Valence-band photoemission and optical absorption in nickel compounds, Phys. Rev. B30 (1984) 957.

[5] P. S. Bagus, G. Pacchioni, F. Parmigiani, Final state effects for the core-level XPS spectra of NiO, Chem. Phys. Lett. 207 (1993) 569.

[6] M. Taguchi, M. Matsunami, Y. Ishida, R. Eguchi, A. Chainami, Y. Takata, M. Yabashi, K. Tamasaku, Y. Nishino, T. Ishikawa, Y. Senba, H. Obashi, S. Shin, Revisiting the valence-band and core-level photoemission spectra of NiO, Phys. Rev. Lett. 100 (2008) 206401.

[7] Q. Yin, A. Gordienko, X. Wan, S. Y. Savrasov, Calculated momentum dependence of Zhang-Rice states in transition metal oxides, Phys. Rev. Lett. 100 (2008) 066406.

[8] D. R. Mullins, S. H. Overbury, D. R. Huntley, Electron spectroscopy of single crystal and polycristalline cerium oxide surfaces, Surf. Sci. 409 (1998) 307.

[9] A. Trovarelli (editor), Catalysis by ceria and related materials, Imperial College Press, London, UK, 2002.

[10] A. Kotani, H. Mizuta, T. Jo, J. C. Parlebas, Theory of core photoemission spectra in CeO_2, Sol. Stat. Commun. 53 (1985) 805.

[11] A. Kotani, T. Jo, J. C. Parlebas, Many-body effects in core-level spectroscopy of rare-earth compounds, Adv. Phys. 37 (1988) 37.

[12] F. M. F. de Groot, X-ray absorption and dichroism of transition metals and their compounds, J. Electron Spectr. Rel. Phenom. 67 (1994) 529.

[13] P. S. Bagus, R. Broer, E. S. Ilton, A new near degeneracy effect for photoemission in transition metals, Chem. Phys. Lett. 394 (2004) 150.

[14] P. S. Bagus, R. Broer, W. A. de Jong, W. C. Nieuwpoort, F. Parmigiani, L. Sangaletti, Atomic many-body effects for the p-shell photoelectron spectra of transition metals, Phys. Rev. Lett. 84 (2000) 2259.

[15] P. S. Bagus, R. Broer, F. Parmigiani, Anomalous electron correlation due to near degeneracy effects: Low-lying ionic states of Ne and Ar, Chem. Phys. Lett. 421 (2006) 148.

[16] P. S. Bagus, R. Broer, E. S. Ilton, Atomic near-degeneracy for photoemission: Generality of 4f excitations, J. Electron Spectrosc. Relat. Phenom. 165 (2008) 46.

[17] E. S. Ilton, P. S. Bagus, Ligand field effects on the multiplet structure of the U 4f XPS of UO_2, Surf. Sci. 602 (2008) 1114.

[18] R. Broer, W. C. Nieuwpoort, Broken orbital-symmetry and the description of hole states in the tetrahedral $[CrO_4]^-$ anion. I. introductory considerations and calculations on oxygen 1s hole states, Chem. Phys. 54 (1981) 291.

[19] J. Cioslowski, Density-driven self-consistent-field method: Density-constrained correlation energies in the helium series, Phys. Rev. A 43 (3) (1991) 1223.

[20] C. de Graaf, R. Broer, W. C. Nieuwpoort, P. S. Bagus, On the role of relaxed charge-transfer excitations: Ni 3s hole states in NiO, Chem. Phys. Lett. 272 (1997) 341.

[21] P. S. Bagus, R. Broer, C. de Graaf, W. C. Nieuwpoort, The electronic structure of NiO for Ni 3s-hole states including full orbital relaxation and localization, J. Electron Spectrosc. Relat. Phenom. 98-99 (1999) 303.

[22] L. Hozoi, A. H. de Vries, R. Broer, C. de Graaf, P. S. Bagus, Ni 3s-hole states in NiO by non-orthogonal configuration interaction, Chem. Phys. 331 (2006) 178.

[23] L. Sangaletti, F. Parmigiani, P. S. Bagus, Sum rule to evaluate the exchange energy in core-level photoemission, Phys. Rev. B 66 (2002) 115106.

[24] T. Åberg, Theory of X-ray satellites, Phys. Rev. 156 (1967) 35.

[25] M. Baron, O. Bondarchuk, D. Stacchiola, S. Shaikhutdinov, H.-J. Freund, Interaction of gold with cerium oxide supports: $CeO_2(111)$ thin films vs CeO_x nanoparticles, J. Phy. Chem. C 113 (2009) 6042.

[26] P. S. Bagus, E. S. Ilton, J. R. Rustad, Ligand-field effects for the $3p$ photoelectron spectra of Cr_2O_3, Phys. Rev. B 69 (2004) 205112.

[27] P. S. Bagus, A. J. Freeman, F. Sasaki, Prediction of new multiplet structure in photoemission experiments, Phys. Rev. Lett. 30 (1973) 850.